Cancer Immunology, Immunotherapy (2021) 70:2657–2668
https://doi.org/10.1007/s00262-020-02827-x

ORIGINAL ARTICLE

Development and validation of a PD-L1/PD-1/CD8 axis-based classifier to predict cancer survival of upper tract urothelial carcinoma after radical nephroureterectomy

Junyu Chen[1,3] · Wenlong Zhong[1,3] · Meng Yang[4] · Weibin Hou[1,3] · Xiaofei Wang[1,3] · Kun Xia[1,3] · Hao Yu[1,3] · Meihua Yang[1,3] · Bingkun Zhou[1,3] · Bo Wang[1,3] · Jian Huang[1,3] · Tianxin Lin[1,2,3]

Received: 1 September 2020 / Accepted: 8 December 2020 / Published online: 19 February 2021

Abstract

The expression status of programmed cell death-ligand 1/programmed cell death 1 (PD-L1/PD-1) and the infiltration of $CD8^+$ T cells in tumor tissues are considered to be related to immunotherapy efficacy and patient prognosis. The purpose of this study is to clarify the prognostic value of the PD-L1/PD-1/CD8 axis, and to develop and validate a comprehensive scoring system based on multiple immune variables to predict cancer survival of upper tract urothelial carcinoma (UTUC) after radical nephroureterectomy (RNU). The immunohistochemical method was used to detect the expression of PD-L1, PD-1, and CD8 in cancer tissues of UTUC patients after RNU. Then, an immunoscore was constructed using the least absolute shrinkage and selection operator (LASSO) Cox regression model in the training cohort ($n = 120$), and it was verified in the validation cohort ($n = 54$). We found that infiltration of PD-$L1^+$ immune cells (ICs), stromal PD-1^+ tumor-infiltrating lymphocytes (TILs), and intratumoral $CD8^+$ TILs was associated with poor overall survival (OS). The immunoscore based on the three immune variables further divided the patients into low- and high-risk groups, and there was a significant difference in the survival rate. A nomogram was constructed by combining tumor-node-metastasis (TNM) stage and immunoscore, and the area under the curve of the receiver-operating characteristic (ROC) (0.78) for predicting 5-year mortality was better than that of the TNM stage (0.70) and immunoscore (0.76). Our results show that the PD-L1/PD-1/CD8 axis-based classifier have potential clinical application to predict cancer survival of UTUC patients after RNU.

Keywords Upper tract urothelial carcinoma · Overall survival · PD-L1 · CD8 · Prognostic classifier

Introduction

Upper tract urothelial carcinoma (UTUC) is a rare malignancy originating from the urinary epithelium of the renal pelvis and ureter, which comprises about 5–10% urothelial carcinoma (UC) cases [1, 2]. Muscle-invasive disease at the time of diagnosis tends to be more common in UTUC than in UC of the bladder (60% vs 25%) [1, 3], partly due to the aggressive phenotype of UTUC. Accordingly, the prognosis of UTUC is relatively poor, with 5-year cancer-specific survival rates of pT2/pT3 and pT4 < 50% and < 10%, respectively [1, 4].

For localized UTUC, although kidney-sparing surgery is indicated in some low-risk cases, radical nephroureterectomy (RNU) with bladder cuff excision is the standard treatment [5]. Similar to the prognosis of UC of the bladder, recent evidence has demonstrated that platinum-based chemotherapy could significantly improve the prognosis of patients with

Junyu Chen, Wenlong Zhong and Meng Yang have contributed equally to this work.

Supplementary Information The online version contains supplementary material available at https://doi.org/10.1007/s00262-020-02827-x.

✉ Bo Wang
wangb43@mail.sysu.edu.cn

✉ Jian Huang
huangj8@mail.sysu.edu.cn

✉ Tianxin Lin
lintx@mail.sysu.edu.cn

Extended author information available on the last page of the article

advanced UTUC [6, 7]. However, only a small proportion of patients can benefit from platinum-based chemotherapy, and the response is inevitably not persistent [8]. Moreover, 20–25% of patients cannot tolerate platinum-based chemotherapy due to impaired renal function, especially after RNU [9, 10]. With the development of cancer immunotherapy, programmed cell death-ligand 1/programmed cell death 1 (PD-L1/PD-1) inhibitors have taken center stage in the treatment of metastatic or locally advanced UC [11]. Previous studies have shown that 22–39% of patients with metastatic UTUC responded to PD-L1/PD-1 inhibitors, which is higher than the percentage of patients with UC of the bladder who responded to PD-L1/PD-1 inhibitors (17–28%) [12]. A therapeutic regimen targeting the PD-L1/PD-1 axis may change the standard of care for patients with UTUC.

The expression of PD-L1/PD-1 in the tumor itself and tumor microenvironment (TME) is considered to be of significance in predicting the response to immunotherapy, as well as patient survival. Recently, researchers have classified the TME into four subtypes according to the PD-L1 expression and density of $CD8^+$ tumor-infiltrating lymphocytes (TILs), which may aid in treatment decision and prognostic prediction [13]. However, few studies have evaluated the PD-L1/PD-1 expression and its prognostic value in UTUC, and it is also largely unknown whether a combination of $CD8^+$ TILs and PD-L1/PD-1 expression could add additional value in stratifying UTUC patients and predicting their immunotherapy response.

Herein, we comprehensively evaluated the expression of PD-L1/PD-1/CD8 axis in UTUC and constructed a PD-L1/PD-1/CD8 axis-based immunoscore, which could accurately predict the survival of UTUC patients in two independent patient cohorts. Furthermore, we integrated the immunoscore with clinicopathologic parameters and developed a prognostic model with a 5-year AUC more than 0.78, which indicates a high clinical application value, and it is worthy of a further study.

Materials and methods

Patients and samples

Our research design is shown in Fig. 1. Patients aged 18 years and older who underwent RNU and were histologically confirmed with UTUC were enrolled. Patients who had distant metastasis at diagnosis, other concurrent malignant tumors, missing clinical information, and missing or unscorable pathological sections, were lost to follow-up and received neoadjuvant chemotherapy were excluded from the study. The patients were separated into training and validation sets randomly in a ratio of 7:3: training cohort ($n = 120$) and validation cohort ($n = 54$).

Clinicopathological data, including gender, age, tumor characteristics, and treatment-related variables, were retrospectively collected. Tumor staging and grading were reviewed by experienced pathologists in a blind manner and classified according to the 2017 tumor-node-metastasis (TNM) classification and the 2004/2016 World Health Organization (WHO) classification. The endpoint of this

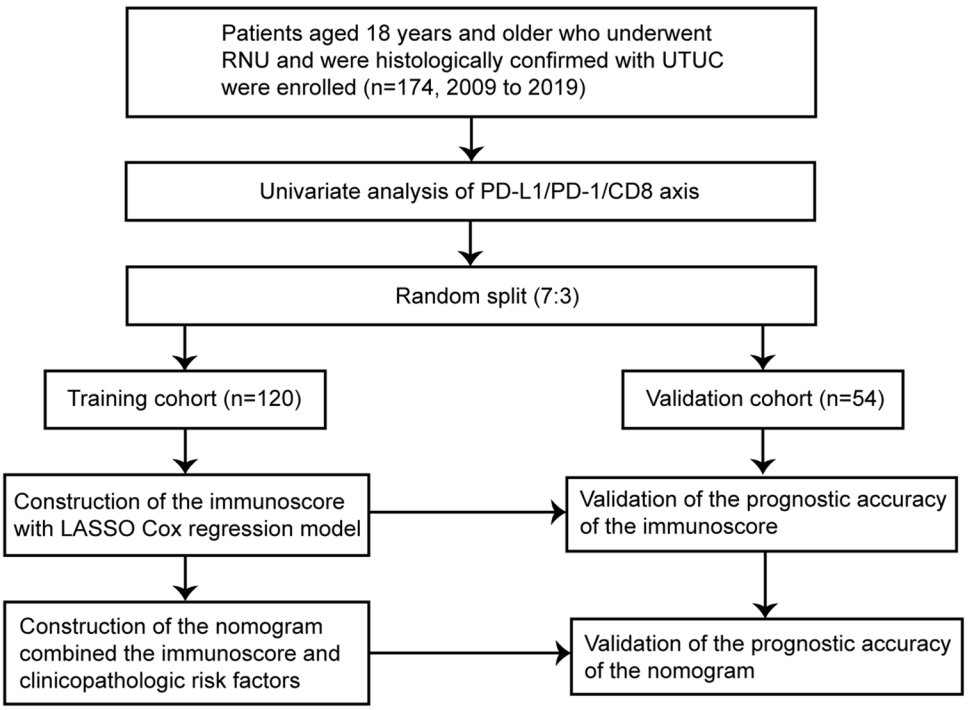

Fig. 1 A flowchart of the study

research was overall survival (OS), which was defined as the period span from the date of the operation to the date of death. Follow-ups included urine cytology and cystoscopy every 3 months and upper tract CT urography once a year. The study was approved by the ethics committee of Sun Yat-sen Memorial Hospital. All enrolled patients signed written informed consent.

Immunohistochemistry

The indirect immunoperoxidase method was used for immunohistochemical (IHC) detection. After dewaxing, rehydration, antigen repair, inactivation of endogenous peroxidase, and blocking of non-specific binding, 4 μm-thick sections were incubated with the following primary antibodies: (anti-PD-L1: 1:400, clone SP142, Spring Bioscience, Fremont, CA, USA; anti-PD-1: 1:100, clone EH33, Cell Signaling Technology, Beverly, MA, USA; anti-CD8: 1:400, clone D8A8Y, Cell Signaling Technology, Beverly, MA, USA) overnight at 4 °C. Then, the slices were incubated with the corresponding secondary antibodies and stained with DAKO EnVision Detection System (DAKO). Finally, the slides were counterstained with hematoxylin and cover-slipped.

Evaluation of immunohistochemical staining

Two independent pathologists who were blinded to clinicopathological and survival data analyzed the tissue sections. PD-L1 expression was evaluated directly under an upright microscope. According to the reference, the staining pattern of PD-L1 in tumor cells (TCs) or immune cells (ICs) is negative or positive when $< 10\%$ or $\geq 10\%$, respectively [14]. $CD8^+$ TILs and PD-1^+ TILs were evaluated by capturing images at five representative high-power fields (×400 magnification, 0.07 mm^2/per field) and counted manually.

In situ immunofluorescence staining

After dewaxing, rehydration, antigen repair, inactivation of endogenous peroxidase, and blocking with 5% bovine serum albumin, sections were incubated with the following primary antibodies: (rabbit anti-human CD8: 1:200, clone D8A8Y, Cell Signaling Technology, Beverly, MA, USA; mouse anti-human PD-1: 1:50, clone UMAB199, ZSGB-BIO, Beijing, China) at 4 °C overnight. Next, the slices were incubated with the secondary antibodies: (Alexa Fluor 594 donkey anti-rabbit, A-21207, Thermo Fisher, Waltham, MA, USA; Alexa Fluor 647 donkey anti-mouse, A-31571, Thermo Fisher, Waltham, MA, USA) at 37 °C for 30 min. Slides were mounted with DAPI mounting medium.

Statistical analysis

Pearson chi-square test or Fisher's exact test was used to compare categorical variables. For continuous variables, Mann–Whitney *U* test was performed. Survival analysis was performed by Kaplan–Meier methods, with *P* values determined by log-rank test. X-tile was used to generate the best cut-off value of PD-1^+ TILs and $CD8^+$ TILs based on the OS data, and according to these cut-off values, the patients were separated into low- and high-risk subgroups. The least absolute shrinkage and selection operator (LASSO) Cox regression model was used to select the immune variables and the coefficients generated by the model were used to develop the immunoscore using the R package glmnet. Multivariate analysis was performed by the multivariate Cox proportional hazard model, including all significant covariates ($P < 0.1$) from the univariate Cox model (forward conditional). The coefficients calculated by the multivariate Cox model were used to generate the nomogram and the calibration curves were drawn using the R package rms. The prognostic authenticity of our model was evaluated by the receiver-operating characteristic (ROC) analysis using survival ROC package. Decision curve analysis was applied to evaluate the clinical utility of the nomogram using the R package dca. $P < 0.05$ was thought to be statistically significant. IBM SPSSV.25.0 and R v.3.4.0 were used for statistical analysis.

Results

Patient characteristics

Table 1 lists the baseline clinicopathologic and immune features of 174 patients with UTUC. The median age at the time of surgery was 65 years (ranging from 33 to 92 years). There were 125 (71.8%) male and 49 (28.2%) female patients. In total, 92 (52.9%) patients were diagnosed with stage 0/0is/I–II disease and 82 (47.1%) patients were diagnosed with stage III–IV. The median OS time was 29.3 months (IQR 11.3–41.8 months). A total of 45 (25.9%) patients died and 42 (24.1%) patients had disease recurrence. Of note, 10 (5.7%) patients had distant metastasis after nephroureterectomy and among these patients, 6 received salvage chemotherapy, 1 received salvage radiotherapy, and 3 received supportive care. There was no significant difference between the training cohort ($n = 120$) and the validation cohort ($n = 54$) in terms of the clinical and immune features (Table 1). With respect to the expression of immune parameters, the representative IHC images for PD-L1, PD-1, and CD8 in UTUC are shown in Fig. 2 and Supplementary Fig. 1. Of note, with PD-L1 as the standard threshold of 10% in intratumoral regions and stromal regions, the positive expression rate of PD-L1 was 42.5% and 39.7%, respectively.

Table 1 Characteristics of patients with upper tract urothelial carcinoma after radical nephroureterectomy [*N* (%)]

Variables	Total ($n=174$)	Training cohort ($n=120$)	Validation cohort ($n=54$)	*P* value
Age (years, median range)	65 (33–92)	64 (36–89)	66 (33–92)	0.158
< 65	88 (50.6%)	65 (54.2%)	23 (42.6%)	
≥ 65	86 (49.4%)	55 (45.8%)	31 (57.4%)	
Gender				0.125
Female	49 (28.2%)	38 (31.7%)	11 (20.4%)	
Male	125 (71.8%)	82 (68.3%)	43 (79.6%)	
Smoking				0.505
No	122 (70.1%)	86 (71.7%)	36 (66.7%)	
Yes	52 (29.9%)	34 (28.3%)	18 (33.3%)	
Side				0.475
Left	94 (54.0%)	67 (55.8%)	27 (50.0%)	
Right	80 (46.0%)	53 (44.2%)	27 (50.0%)	
Location				0.655
Ureter	72 (41.4%)	51 (42.5%)	21 (38.9%)	
Pelvic	102 (58.6%)	69 (57.5%)	33 (61.1%)	
Tumor size				0.126
< 2 cm	27 (15.5%)	22 (18.3%)	5 (9.3%)	
≥ 2 cm	147 (84.5%)	98 (81.7%)	49 (90.7%)	
Multifocality				0.890
Absence	146 (83.9%)	101 (84.2%)	45 (83.3%)	
Presence	28 (16.1%)	19 (15.8%)	9 (16.7%)	
CKD stage				0.770
Stage 1	110 (63.2%)	75 (62.5%)	35 (64.8%)	
Stage 2–5	64 (36.8%)	45 (37.5%)	19 (35.2%)	
Tumor grade				0.197
G1–2	25 (14.4%)	20 (16.7%)	5 (9.3%)	
G3	149 (85.6%)	100 (83.3%)	49 (90.7%)	
TNM stage				0.883
0/0is/I–II	92 (52.9%)	63 (52.5%)	29 (53.7%)	
III–IV	82 (47.1%)	57 (47.5%)	25 (46.3%)	
Regional lymphadenectomy				0.864
Absence	147 (84.5%)	101 (84.2%)	46 (85.2%)	
Presence	27 (15.5%)	19 (15.8%)	8 (14.8%)	
Adjuvant chemotherapy				0.292
Absence	140 (80.5%)	94 (78.3%)	46 (85.2%)	
Presence	34 (19.5%)	26 (21.7%)	8 (14.8%)	
PD-L1 TCs				0.315
Negative	100 (57.5%)	72 (60.0%)	28 (51.9%)	
Positive	74 (42.5%)	48 (40.0%)	26 (48.1%)	
PD-L1 ICs				0.595
Negative	105 (60.3%)	74 (61.7%)	31 (57.4%)	
Positive	69 (39.7%)	46 (38.3%)	23 (42.6%)	
INT PD-1$^+$ TILs				0.548
Low	94 (54.0%)	63 (52.5%)	31 (57.4%)	
High	80 (46.0%)	57 (47.5%)	23 (42.6%)	
ST PD-1$^+$ TILs				0.373
Low	131 (75.3%)	88 (73.3%)	43 (79.6%)	
High	43 (24.7%)	32 (26.7%)	11 (20.4%)	
INT CD8$^+$ TILs				0.278
Low	99 (56.9%)	65 (54.2%)	34 (63.0%)	
High	75 (43.1%)	55 (45.8%)	20 (37.0%)	
ST CD8$^+$ TILs				0.212
Low	114 (65.5%)	75 (62.5%)	39 (72.2%)	
High	60 (34.5%)	45 (37.5%)	15 (27.8%)	

PD-L1 programmed cell death-ligand 1, *PD-1* programmed cell death 1, *TILs* tumor infiltrating lymphocytes, *TCs* tumor cells, *ICs* immune cells, *INT* Intratumoral regions, *ST* stromal regions; *P* values were determined using the Pearson chi-square test or Fisher's exact test

Predictive value of the PD-L1/PD-1/CD8 axis in prognosis

Kaplan–Meier test showed that PD-L1$^+$ ICs and high stromal PD-1$^+$ TILs were correlated with poor OS ($P=0.0024$ and $P=0.038$, respectively) (Fig. 3b, d). However, PD-L1 expressed by TCs and intratumoral PD-1$^+$ TILs were not correlated with the OS of the UTUC patients (Fig. 3a, c). Of note, previous studies dispute the prognostic value of CD8$^+$ TILs in UC [15, 16]. In our study, patients with high intratumoral CD8$^+$ TILs showed a significant decrease in overall survival compared with patients in the low subgroup ($P=0.017$), while there was no significant difference in OS between the high subgroup and low subgroup of stromal CD8$^+$ TILs (Fig. 3e, f).

By analyzing IHC images in serial sections, we found that the positively stained regions of CD8 and PD-1 overlapped, especially in patients with high densities of both CD8$^+$ TILs and PD-1$^+$ TILs (Fig. 4a–d). Pearson tests showed that the density of CD8$^+$ TILs and the density of PD-1$^+$ TILs were significantly positive correlated in both stromal regions and intratumoral regions (intratumoral regions: $r=0.540$, $P<0.001$; stromal regions: $r=0.454$, $P<0.001$) (Fig. 4e, f). We further confirmed the results by evaluating the transcript data from the Gene Expression Omnibus (GEO) database (GSE134292; Supplementary Fig. 2). Double immunofluorescent staining showed PD-1 and CD8 co-expression (Fig. 4g–j). This may explain the contradictory value of CD8$^+$ TILs in prognosis prediction.

Development and validation of immunoscore of UTUC

To investigate the prognostic value of the PD-L1/PD-1/CD8 axis, we calculated the immunoscore for each patient using

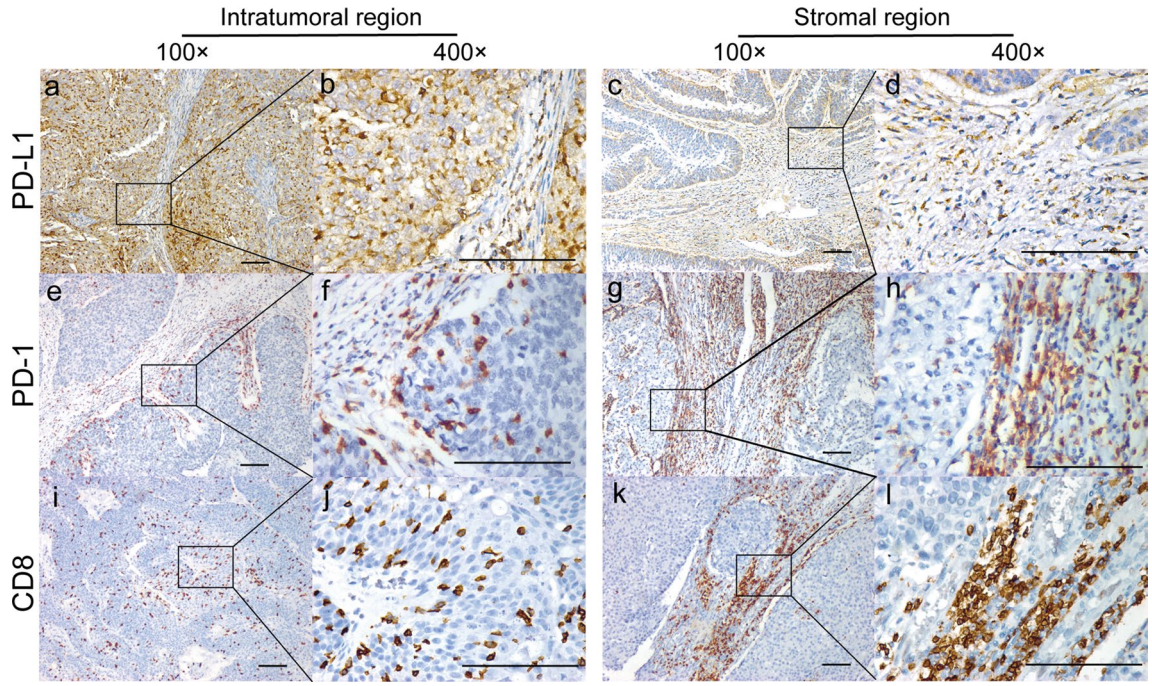

Fig. 2 Representative images of PD-L1, PD-1, and CD8 staining in UTUC. Samples are shown at × 100 or × 400 (scale bar 100 μm) original magnification. Positive expression of PD-L1 in the intratumoral region (**a**, **b**) and stromal region (**c**, **d**). High-risk group of PD-1$^+$ TILs in the intratumoral region (**e**, **f**) and stromal region (**g**, **h**). High-risk group of CD8$^+$ TILs in the intratumoral region (**i**, **j**) and stromal region (**k**, **l**)

the LASSO Cox model in the training cohort (Fig. 5a, b). The formula for immunoscore was based on the status of the following three immune variables:

Immunoscore = (0.7879 × PD-L1 ICs status) + (0.6011 × Stromal PD-1$^+$ TILs status) + (0.2422 × Intratumoral CD8$^+$ TILs status).

In the training cohort, we assign patients to high- and low-risk groups based on the optimal cut-off value of the immunoscore generated by X-tile. The low-risk group was significantly associated with the improvement of OS ($P = 0.0042$) (Fig. 5c). Then, the cut-off value obtained from the training set was applied to the validation set. Consistently, the patients in high-risk group had shorter OS than those in low-risk group in the validation cohort ($P = 0.024$) (Fig. 5d).

Next, we evaluated the predictive value of the immunoscore using time-dependent ROC analysis. The AUC values of the immunoscore at 1, 3, and 5 years were 0.67 (95% CI 0.52–0.82), 0.66 (95% CI 0.52–0.79), and 0.74 (95% CI 0.62–0.88) in the training cohort, and 0.80 (95% CI 0.59–0.93), 0.71 (95% CI 0.60–0.90), and 0.75 (95% CI 0.61–0.93) in the validation cohort (Fig. 5e, f). Subgroup analysis found that patients in the low stage 0/0is/I-II or high stage III–IV could be further divided into high and low-risk subgroups by the immunoscore (Supplementary Fig. 3). The immunoscore may provide more accurate prognosis and can be complementary to the TNM staging system for patients with UTUC.

Nomogram based on the combination of immunoscore and clinicopathologic parameters

To establish a more sensitive survival prediction model for patients with UTUC, we established a comprehensive prognostic model based on the combination of immunoscore and clinicopathologic parameters. After multivariable adjustment for clinicopathological factors, immunoscore and TNM stage remained strong independent prognostic markers for OS in the training set (Supplementary Table 1). Then, we constructed a nomogram combining the immunoscore and TNM stage to predict the 5-year OS (Fig. 6a). The calibration curves indicated favorable accordance between the nomogram-predicted 5-year OS and the observed 5-year OS in the training cohort (C-index 0.845, 95%CI 0.781 to 0.909), the validation cohort (C-index 0.804, 95% CI 0.713 to 0.895), and the combined cohort (C-index 0.830, 95% CI 0.776 to 0.884) (Fig. 6b). Decision curve analysis displayed well positive net benefits in both cohorts (Fig. 6c), revealing that the nomogram had good clinical application in predicting 5-year OS.

Further survival analysis showed that patients in high-risk subgroup divided by the nomogram had worse OS

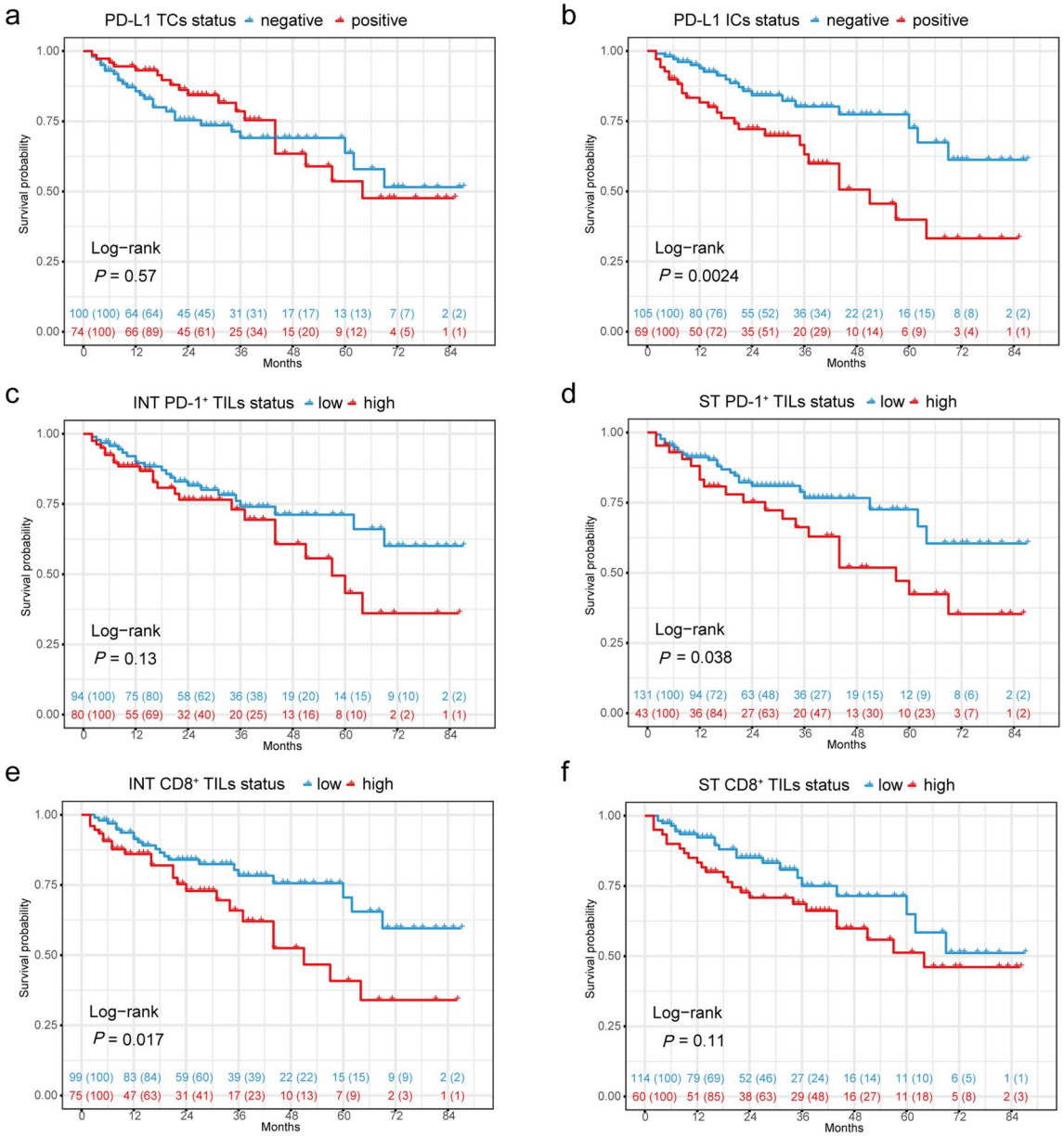

Fig. 3 Kaplan–Meier overall survival curves for patients with UTUC stratified by (**a**, **b**) PD-L1 TCs status and PD-L1 ICs status, (**c**, **d**) PD-1$^+$ TILs status in the intratumoral and stromal regions, and (**e**, **f**) CD8$^+$ TILs status in the intratumoral and stromal regions. *P* values were determined using the log-rank test

than low-risk subgroup in the training, validation, and combined cohorts (Fig. 7a–c). ROC analysis was used to compare the sensitivity and specificity of the nomogram with TNM staging or immunoscore alone. In the training set, the prognostic value of immunoscore combined with TNM staging in OS (AUC of 0.78, 95% CI 0.64–0.93) was better than that of TNM staging (AUC of 0.67, 95% CI 0.53–0.87) or immunoscore model (AUC of 0.74, 95% CI 0.62–0.88) alone, which was further verified in the validation set (Fig. 7d, e). Furthermore, we performed the ROC analysis in the combined set, and the AUC of the nomogram at 5 years was 0.78 (95% CI 0.70–0.88) (Fig. 7f).

Discussion

Despite the encouraging results of immune checkpoint inhibitors (ICIs) in UTUCs, limited data are available with regard to the correlation and prognostic role of the entire PD-L1/PD-1/CD8 axis of UTUC. To address these limitations, we comprehensively assessed the expression of CD8$^+$ TILs and

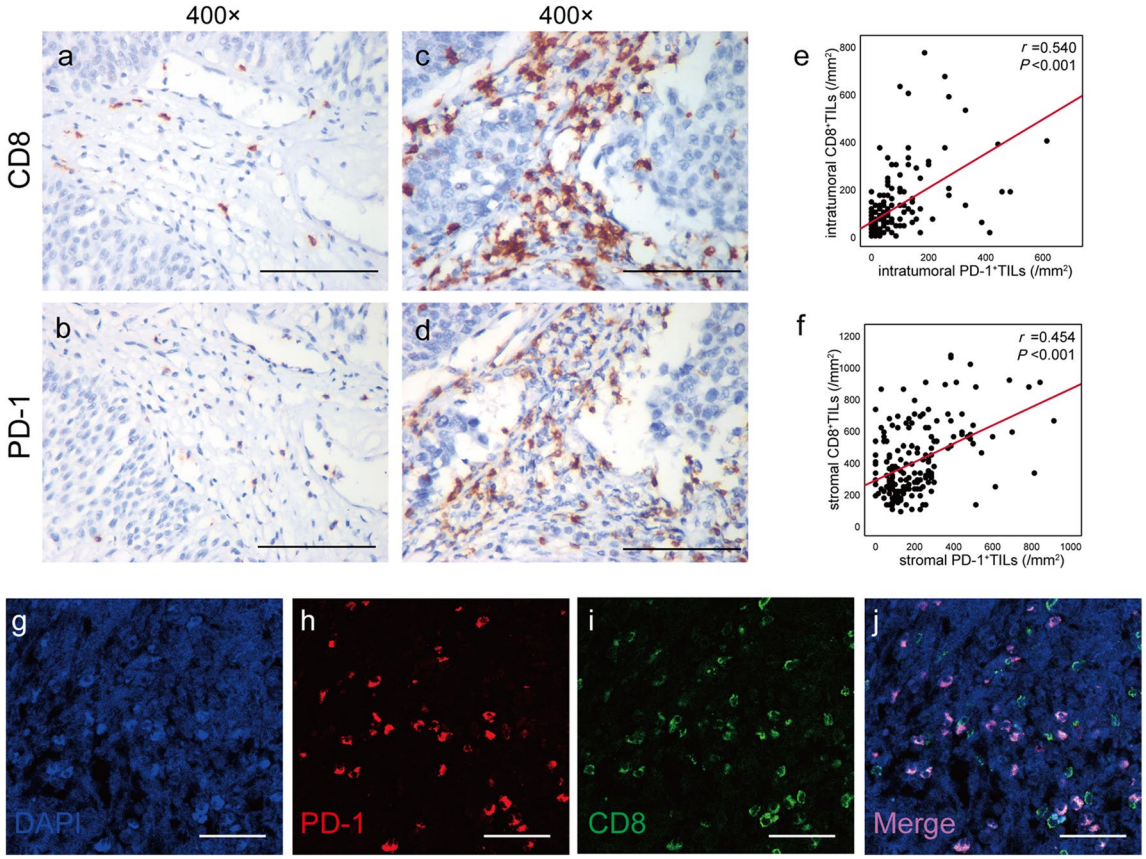

Fig. 4 Representative images of CD8 (**a**, **c**) and PD-1 (**b**, **d**) staining in tumor serial sections. Samples are shown at × 400 (scale bar 100 μm) original magnification. Analyses of the correlation between the PD-1$^+$ TILs and CD8$^+$ TILs in the intratumoral and stromal regions (**e**, **f**). Significance was assessed by Pearson correlation. Representative images of in situ double immunofluorescent staining by confocal analysis (scale bar 50 μm) (**g**–**j**)

PD-L1/PD-1, and developed a PD-L1/PD-1/CD8 axis-based immunoscore in UTUC patients. In our study, we found that PD-L1$^+$ ICs, stromal PD-1$^+$ TILs, and intratumoral CD8$^+$ TILs were associated with poor prognosis. Moreover, we developed an immunoscore based on the axis, and the 5-year mortality rate predicted by ROC analysis was better than that of the TNM system. To our knowledge, this is the first study to comprehensively characterize the expression of the PD-L1/PD-1/CD8 axis in UTUC patients. The immunoscore developed for UTUC based on immune infiltration and function could be integrated into the current TNM staging system to provide additional prognostic information.

Previous studies have shown conflicting results concerning the prognostic value of PD-L1 and its predictive value in immunotherapy response in UTUC. For instance, Skala et al. [17] found that PD-L1 expression in UTUC was not associated with cancer-specific survival. On the other hand, Krabbe et al. [18] have identified PD-L1 positivity as a favorable predictor of survival in cases of organ confined UTUC, while Miyama et al. [19] believed that PD-L1 expression was an adverse predictor for survival in their high-platelet UTUC subgroup. PD-L1 is expressed on both tumor cells and immune cells, and its cell-specific expression might have different prognostic meanings. The expression of PD-L1 on ICs seems to be a more predictive biomarker for immunotherapy in urothelial carcinoma [20]. It has been reported that stromal PD-L1 is mainly expressed on antigen-presenting cells, such as macrophages [21, 22], which exert immunosuppressive function by inducing T-cell apoptosis and up-regulating the expression of multiple cytokines like interleukin-10 [23]. In our study, survival analysis showed that an increasing number of PD-L1$^+$ ICs, rather than PD-L1$^+$ TCs, were associated with poor OS, which may partly explain the result of clinical study (NCT02108652) [24].

Infiltration of CD8$^+$ T cells has been proved to be related to a favorable prognosis of many cancers [25–27], but some studies have put forward opposite views. Hsu et al. [28] found that an increase in intratumoral PD-1$^+$ CD8$^+$ T cells predicted a poor prognosis of nasopharyngeal carcinoma. Wen et al. [29] found that the OS of gastric cancer patients with $CD8_{More}PD\text{-}1_{low}$ was significantly better than that of

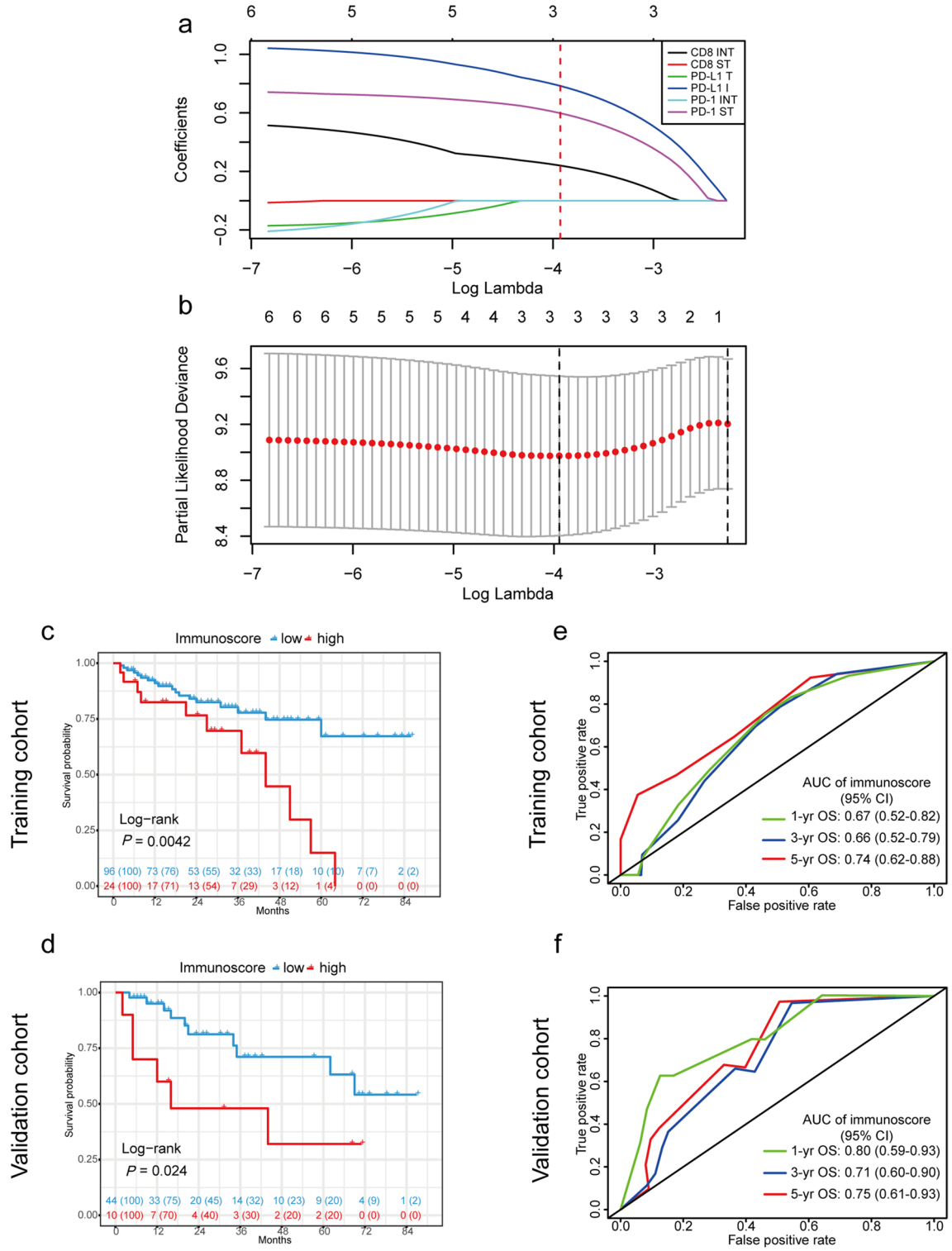

Fig. 5 **a** LASSO coefficient profiles of the six immune features. CD8 INT, intratumoral CD8$^+$ TILs status; CD8 ST, stromal CD8$^+$ TILs status; PD-L1 T, PD-L1 TCs status; PD-L1 I, PD-L1 ICs status; PD-1 INT, intratumoral PD-1$^+$ TILs status; PD-1 ST, stromal PD-1$^+$ TILs status. **b** Tuning parameter (λ) selection in the LASSO model used tenfold cross-validation via minimum criteria. **c**, **d** Kaplan–Meier curves for overall survival between the immunoscore high- and low-risk groups in the training and validation cohorts. **e**, **f** ROC analysis of 1-, 3-, and 5-year survival rates based on immunoscore in the training and validation cohorts

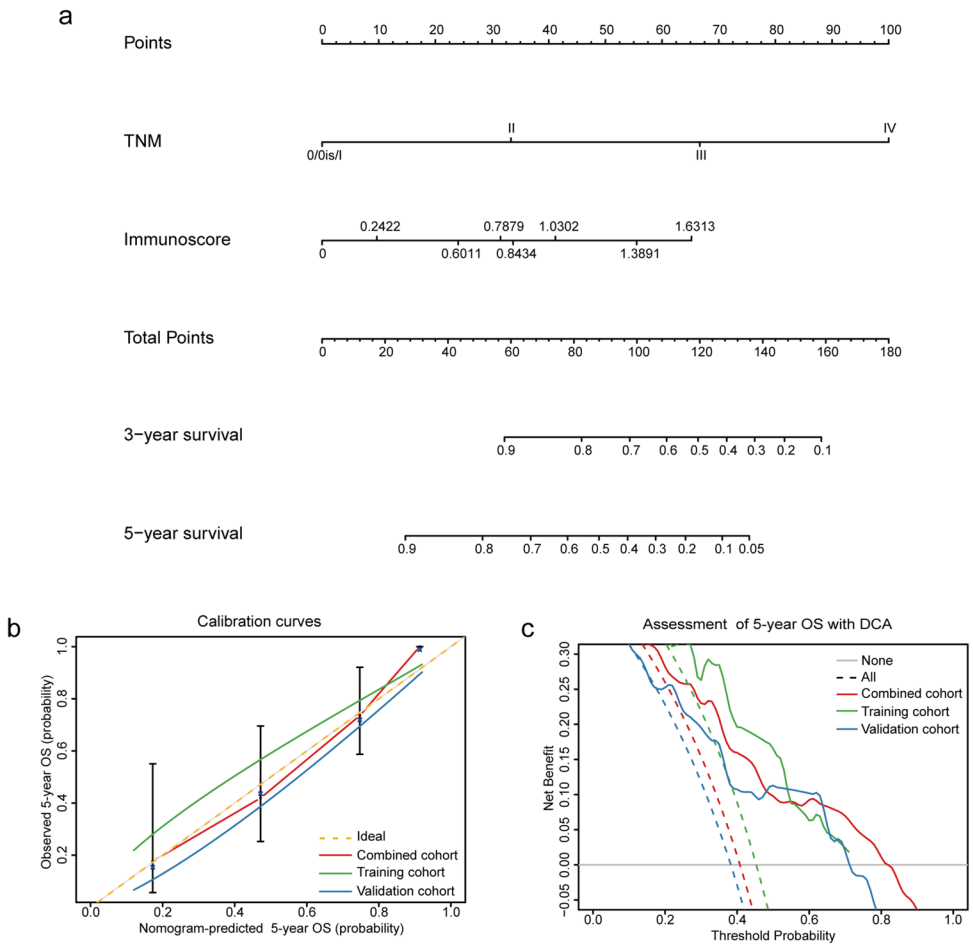

Fig. 6 **a** Nomogram for predicting 3/5-year overall survival of patients with UTUC. **b** The calibration plots for predicting overall survival at the 5-year point in the training cohort, validation cohort, and combined cohort. **c** Decision curve analysis for the nomogram model in the training cohort, validation cohort, and combined cohort

$CD8_{More}PD\text{-}1_{high}$ patients, suggesting that the prognosis of patients should be judged by the combination of CD8 and PD-1. The prognosis of $CD8^+$ T cells in UC is controversial, which may be related to considering only the number and location of lymphocyte infiltration while neglecting the function of these immune cells. Previous studies performed in our center have shown that $CD8^+$ TIL in bladder cancer is associated with poor prognosis [15], and PD-1 expression in T-cell subsets as well as T-cell topographic microlocalizations could provide additional prognostic value [30]. In this study, we found that there was a significant positive correlation between density of $CD8^+$ TILs and density of $PD\text{-}1^+$ TILs in UTUC, suggesting that $CD8^+$ TILs in UTUC TME were depleted. Intratumoral $CD8^+$ TILs were associated with poor OS, and stromal $CD8^+$ TILs caused no significant difference in OS between the low- and high-risk groups, which may suggest that intratumoral $CD8^+$ TILs play a more decisive role in tumor progression.

With our rapid accrual of knowledge in tumor biology, integration of molecular and TME biomarkers with TNM staging has been the current focus to improve our ability to perform risk stratification of cancer patients. Particularly, the rise of immunotherapy for various cancers, including UTUC, warrants studies characterizing its immune profiles directly relevant to immunotherapy responses [31]. In this study, we have developed a comprehensive immune scoring system, including cytotoxic T-cell infiltration (CD8), T-cell function (PD-1), and immune checkpoint (PD-L1). These three factors represent the backbone of cancer immunology. The results showed that this immune scoring system could serve as an independent biomarker to predict the prognosis of UTUC patients, and it also has the potential to predict UTUC response to ICIs.

This study has several limitations. First, this is a retrospective study and selection bias is inevitable. Second, although the specificity of the antibodies used in this study has been confirmed in various studies [32–34], the antibody selection and evaluation methods of IHC staining for the PD-L1/PD-1/CD8 axis may have affected the results. For instance, PD-L1mAb (MPDL3280A), which is the widely used drug Atezolizumab, prefers to detect the expression of PD-L1 on tumor-infiltrating ICs in UC, rather than detecting the expression of PD-L1 on tumor cells [35]. Third, the role of our immune score in predicting UTUC response to ICIs has not been validated and a prospective multicenter study is required to test our hypothesis.

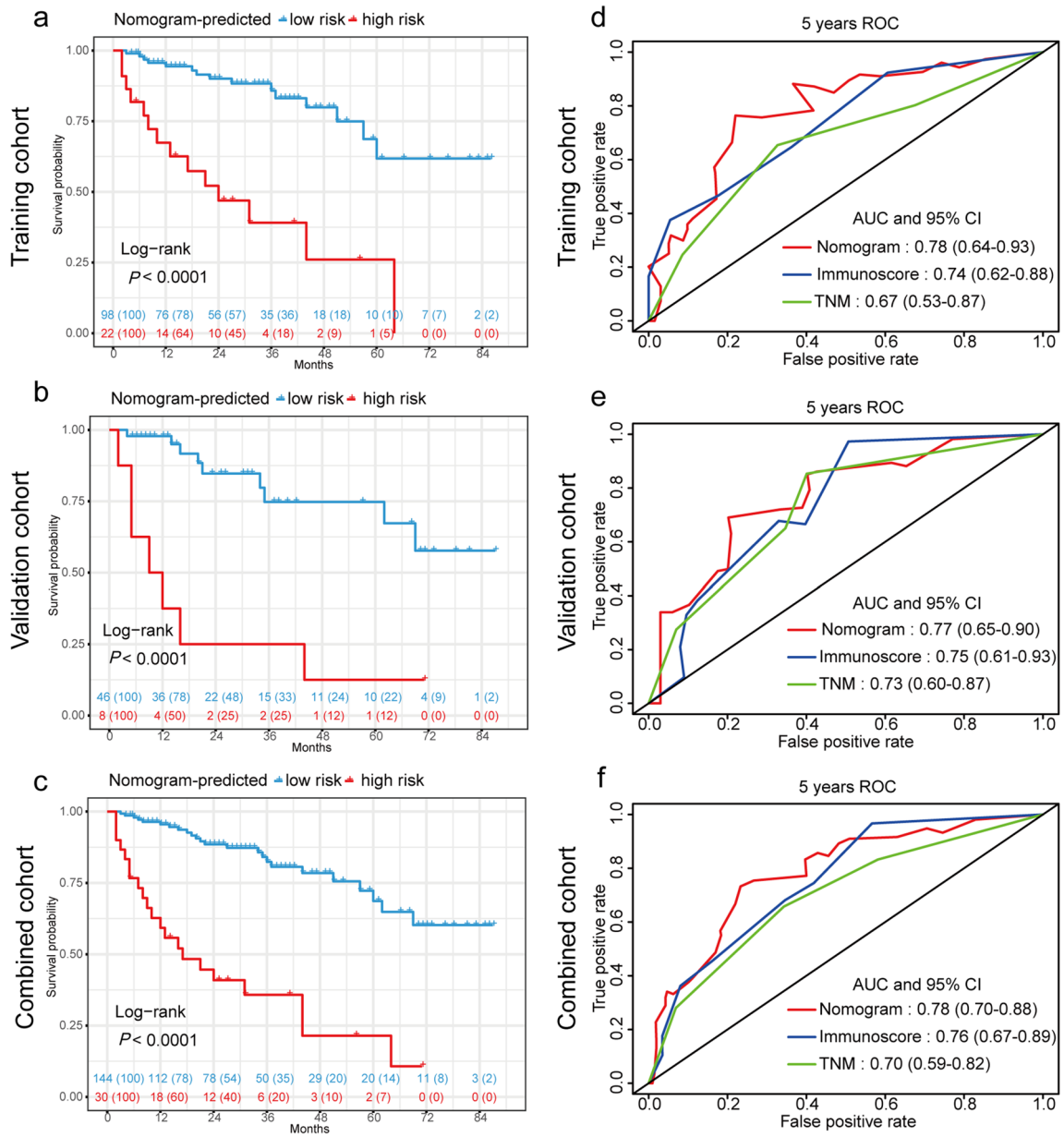

Fig. 7 Kaplan–Meier curves for overall survival between the nomogram high- and low-risk groups in the **a** training cohort, **b** validation cohort, and **c** combined cohort. ROC analysis of the 5-year survival rate based on nomogram, immunoscore, and TNM stage in the **d** training cohort, **e** validation cohort, and **f** combined cohort

In summary, our results demonstrate that PD-L1$^+$ ICs, stromal PD-1$^+$ TILs, and intratumoral CD8$^+$ TILs are associated with poor prognosis in patients with UTUC. Furthermore, the PD-L1/PD-1/CD8 axis-based immunoscore can effectively predict the survival and add prognostic value to TNM staging. Our model may facilitate the prognostic prediction, but more investigations in larger and multi-institutional cohorts are needed.

Author contributions JYC and WLZ designed the study and wrote the manuscript; MY and KX collected and analyzed the clinical data and pathological review; WBH and XFW performed immunohistochemistry and immunofluorescence staining; HY, MHY, BKZ, and BW modified and revised the manuscript; JH and TXL performed the surgeries and made important revisions to the manuscript. All authors have approved the submission of this manuscript.

Funding This study was supported by the National Natural Science Foundation of China (Grant nos. 81772719, 81825016, 81902586,

81961128027); Guangdong Basic and Applied Basic Research Foundation (2020A1515011312); China Postdoctoral Science Foundation (2018M640862, 2019M653196); Fundamental Research Funds for the Central Universities (19ykpy116, 19ykpy117); Key Laboratory of Malignant Tumor Gene Regulation and Target Therapy of Guangdong Higher Education Institutes, Sun-Yat-Sen University (Grant no. KLB09001); Key Laboratory of Malignant Tumor Molecular Mechanism and Translational Medicine of Guangzhou Bureau of Science and Information Technology (Grant no. 013-163).

Compliance with ethical standards

Conflict of interest The authors declare that they have no competing interests.

References

1. Rouprêt M, Babjuk M, Burger M, Capoun O, Cohen D, Compérat EM, Cowan NC, Dominguez-Escrig JL, Gontero P, Hugh Mostafid A, Palou J, Peyronnet B, Seisen T, Soukup V, Sylvester RJ, Rhijn B, Zigeuner R, Shariat SF (2020) European Association of Urology Guidelines on Upper Urinary Tract Urothelial Carcinoma: 2020 update. Eur Urol. https://doi.org/10.1016/j.eururo.2020.05.042
2. Siegel RL, Miller KD, Jemal A (2019) Cancer statistics, 2019. CA Cancer J Clin 69(1):7–34. https://doi.org/10.3322/caac.21551
3. Margulis V, Shariat SF, Matin SF, Kamat AM, Zigeuner R, Kikuchi E, Lotan Y, Weizer A, Raman JD, Wood CG (2009) Outcomes of radical nephroureterectomy: a series from the upper tract urothelial carcinoma collaboration. Cancer 115(6):1224–1233. https://doi.org/10.1002/cncr.24135
4. Lughezzani G, Burger M, Margulis V, Matin SF, Novara G, Roupret M, Shariat SF, Wood CG, Zigeuner R (2012) Prognostic factors in upper urinary tract urothelial carcinomas: a comprehensive review of the current literature. Eur Urol 62(1):100–114. https://doi.org/10.1016/j.eururo.2012.02.030
5. Seisen T, Peyronnet B, Dominguez-Escrig JL, Bruins HM, Yuan CY, Babjuk M, Böhle A, Burger M, Compérat EM, Cowan NC, Kaasinen E, Palou J, van Rhijn BW, Sylvester RJ, Zigeuner R, Shariat SF, Rouprêt M (2016) Oncologic outcomes of kidney-sparing surgery versus radical nephroureterectomy for upper tract urothelial carcinoma: a systematic review by the EAU non-muscle invasive bladder cancer guidelines panel. Eur Urol 70(6):1052–1068. https://doi.org/10.1016/j.eururo.2016.07.014
6. Leow JJ, Martin-Doyle W, Fay AP, Choueiri TK, Chang SL, Bellmunt J (2014) A systematic review and meta-analysis of adjuvant and neoadjuvant chemotherapy for upper tract urothelial carcinoma. Eur Urol 66(3):529–541. https://doi.org/10.1016/j.eururo.2014.03.003
7. Seisen T, Krasnow RE, Bellmunt J, Rouprêt M, Leow JJ, Lipsitz SR, Vetterlein MW, Preston MA, Hanna N, Kibel AS, Sun M, Choueiri TK, Trinh QD, Chang SL (2017) Effectiveness of adjuvant chemotherapy after radical nephroureterectomy for locally advanced and/or positive regional lymph node upper tract urothelial carcinoma. J Clin Oncol 35(8):852–860. https://doi.org/10.1200/jco.2016.69.4141
8. Patel MR, Ellerton J, Infante JR, Agrawal M, Gordon M, Aljumaily R, Britten CD, Dirix L, Lee KW, Taylor M, Schöffski P, Wang D, Ravaud A, Gelb AB, Xiong J, Rosen G, Gulley JL, Apolo AB (2018) Avelumab in metastatic urothelial carcinoma after platinum failure (JAVELIN Solid Tumor): pooled results from two expansion cohorts of an open-label, phase 1 trial. Lancet Oncol 19(1):51–64. https://doi.org/10.1016/s1470-2045(17)30900-2
9. Fang D, Zhang Q, Li X, Qian C, Xiong G, Zhang L, Chen X, Zhang X, Yu W, He Z, Zhou L (2014) Nomogram predicting renal insufficiency after nephroureterectomy for upper tract urothelial carcinoma in the Chinese population: exclusion of ineligible candidates for adjuvant chemotherapy. Biomed Res Int 2014:529186. https://doi.org/10.1155/2014/529186
10. Xiong G, Chen X, Li X, Fang D, Zhang L, Yang L, Zhang L, Yao L, He Z, Zhou L (2014) Prevalence and factors associated with baseline chronic kidney disease in China: a 10-year study of 785 upper urinary tract urothelial carcinoma patients. Journal of the Formosan Medical Association = Taiwan yi zhi 113(8):521–526. https://doi.org/10.1016/j.jfma.2013.04.001
11. EAU Guidelines. Edn. Presented at the EAU Annual Congress Barcelona 2019. ISBN 978-94-92671-04-2
12. Yang HY, Yang CC, Wu CY, Wang LJ, Lu KL (2019) Aristolochic acid and immunotherapy for urothelial carcinoma: directions for unmet needs. Int J Mol Sci. https://doi.org/10.3390/ijms20133162
13. Teng MW, Ngiow SF, Ribas A, Smyth MJ (2015) Classifying cancers based on T-cell Infiltration and PD-L1. Cancer Res 75(11):2139–2145. https://doi.org/10.1158/0008-5472.Can-15-0255
14. Zhu J, Armstrong AJ, Friedlander TW, Kim W, Pal SK, George DJ, Zhang T (2018) Biomarkers of immunotherapy in urothelial and renal cell carcinoma: PD-L1, tumor mutational burden, and beyond. J Immunotherapy Cancer 6(1):4. https://doi.org/10.1186/s40425-018-0314-1
15. Wang B, Pan W, Yang M, Yang W, He W, Chen X, Bi J, Jiang N, Huang J, Lin T (2019) Programmed death ligand-1 is associated with tumor infiltrating lymphocytes and poorer survival in urothelial cell carcinoma of the bladder. Cancer Sci 110(2):489–498. https://doi.org/10.1111/cas.13887
16. Sharma P, Shen Y, Wen S, Yamada S, Jungbluth AA, Gnjatic S, Bajorin DF, Reuter VE, Herr H, Old LJ, Sato E (2007) CD8 tumor-infiltrating lymphocytes are predictive of survival in muscle-invasive urothelial carcinoma. Proc Natl Acad Sci USA 104(10):3967–3972. https://doi.org/10.1073/pnas.0611618104
17. Skala SL, Liu TY, Udager AM, Weizer AZ, Montgomery JS, Palapattu GS, Siddiqui J, Cao X, Fields K, Abugharib AE, Soliman M, Hafez KS, Miller D, Lee CT, Alva A, Chinnaiyan AM, Morgan TM, Spratt DE, Jiang H, Mehra R (2017) Programmed death-ligand 1 expression in upper tract urothelial carcinoma. Eur Urol Focus 3(4–5):502–509. https://doi.org/10.1016/j.euf.2016.11.011
18. Krabbe LM, Heitplatz B, Preuss S, Hutchinson RC, Woldu SL, Singla N, Boegemann M, Wood CG, Karam JA, Weizer AZ, Raman JD, Remzi M, Rioux-Leclercq N, Haitel A, Rapoport LM, Glybochko PV, Roscigno M, Bolenz C, Bensalah K, Sagalowsky AI, Shariat SF, Lotan Y, Xylinas E, Margulis V (2017) Prognostic Value of PD-1 and PD-L1 expression in patients with high grade upper tract urothelial carcinoma. J Urol 198(6):1253–1262. https://doi.org/10.1016/j.juro.2017.06.086
19. Miyama Y, Morikawa T, Miyakawa J, Koyama Y, Kawai T, Kume H, Fukayama M (2018) The prognostic value of PD-L1 expression in upper tract urothelial carcinoma varies according to platelet count. Cancer Med 7(9):4330–4338. https://doi.org/10.1002/cam4.1686
20. Havel JJ, Chowell D, Chan TA (2019) The evolving landscape of biomarkers for checkpoint inhibitor immunotherapy. Nat Rev Cancer 19(3):133–150. https://doi.org/10.1038/s41568-019-0116-x
21. Gatalica Z, Snyder C, Maney T, Ghazalpour A, Holterman DA, Xiao N, Overberg P, Rose I, Basu GD, Vranic S, Lynch HT, Von Hoff DD, Hamid O (2014) Programmed cell death 1 (PD-1) and its ligand (PD-L1) in common cancers and their correlation with molecular cancer type. Cancer Epidemiol Biomark

Prev 23(12):2965–2970. https://doi.org/10.1158/1055-9965.Epi-14-0654
22. Cha JH, Chan LC, Li CW, Hsu JL, Hung MC (2019) Mechanisms controlling PD-L1 expression in cancer. Mol Cell 76(3):359–370. https://doi.org/10.1016/j.molcel.2019.09.030
23. Kubota K, Moriyama M, Furukawa S, Rafiul H, Maruse Y, Jinno T, Tanaka A, Ohta M, Ishiguro N, Yamauchi M, Sakamoto M, Maehara T, Hayashida JN, Kawano S, Kiyoshima T, Nakamura S (2017) CD163 (+)CD204 (+) tumor-associated macrophages contribute to T cell regulation via interleukin-10 and PD-L1 production in oral squamous cell carcinoma. Sci Rep 7(1):1755. https://doi.org/10.1038/s41598-017-01661-z
24. Rosenberg JE, Hoffman-Censits J, Powles T, van der Heijden MS, Balar AV, Necchi A, Dawson N, O'Donnell PH, Balmanoukian A, Loriot Y, Srinivas S, Retz MM, Grivas P, Joseph RW, Galsky MD, Fleming MT, Petrylak DP, Perez-Gracia JL, Burris HA, Castellano D, Canil C, Bellmunt J, Bajorin D, Nickles D, Bourgon R, Frampton GM, Cui N, Mariathasan S, Abidoye O, Fine GD, Dreicer R (2016) Atezolizumab in patients with locally advanced and metastatic urothelial carcinoma who have progressed following treatment with platinum-based chemotherapy: a single-arm, multicentre, phase 2 trial. Lancet (London, England) 387(10031):1909–1920. https://doi.org/10.1016/s0140-6736(16)00561-4
25. Sato E, Olson SH, Ahn J, Bundy B, Nishikawa H, Qian F, Jungbluth AA, Frosina D, Gnjatic S, Ambrosone C, Kepner J, Odunsi T, Ritter G, Lele S, Chen YT, Ohtani H, Old LJ, Odunsi K (2005) Intraepithelial CD8+ tumor-infiltrating lymphocytes and a high CD8+/regulatory T cell ratio are associated with favorable prognosis in ovarian cancer. Proc Natl Acad Sci USA 102(51):18538–18543. https://doi.org/10.1073/pnas.0509182102
26. Yamada N, Oizumi S, Kikuchi E, Shinagawa N, Konishi-Sakakibara J, Ishimine A, Aoe K, Gemba K, Kishimoto T, Torigoe T, Nishimura M (2010) CD8+ tumor-infiltrating lymphocytes predict favorable prognosis in malignant pleural mesothelioma after resection. Cancer Immunol Immunotherapy CII 59(10):1543–1549. https://doi.org/10.1007/s00262-010-0881-6
27. Ye SL, Li XY, Zhao K, Feng T (2017) High expression of CD8 predicts favorable prognosis in patients with lung adenocarcinoma: a cohort study. Medicine 96(15):e6472. https://doi.org/10.1097/md.0000000000006472
28. Hsu MC, Hsiao JR, Chang KC, Wu YH, Su IJ, Jin YT, Chang Y (2010) Increase of programmed death-1-expressing intratumoral CD8 T cells predicts a poor prognosis for nasopharyngeal carcinoma. Modern Pathol 23(10):1393–1403. https://doi.org/10.1038/modpathol.2010.130
29. Wen T, Wang Z, Li Y, Li Z, Che X, Fan Y, Wang S, Qu J, Yang X, Hou K, Zhou W, Xu L, Li C, Wang J, Liu J, Chen L, Zhang J, Qu X, Liu Y (2017) A Four-factor immunoscore system that predicts clinical outcome for stage II/III gastric cancer. Cancer Immunol Res 5(7):524–534. https://doi.org/10.1158/2326-6066.Cir-16-0381
30. Hou W, Xue M, Shi J, Yang M, Zhong W, Fan X, Zeng H, Lai Y, Huang J, Wang B, Lin T (2020) PD-1 topographically defines distinct T cell subpopulations in urothelial cell carcinoma of the bladder and predicts patient survival. Urol Oncol 38(8):685.e681-685.e610. https://doi.org/10.1016/j.urolonc.2020.04.009
31. van Dijk N, Funt SA, Blank CU, Powles T, Rosenberg JE, van der Heijden MS (2019) The Cancer Immunogram as a Framework for Personalized Immunotherapy in Urothelial Cancer. Eur Urol 75(3):435–444. https://doi.org/10.1016/j.eururo.2018.09.022
32. Shukuya T, Carbone DP (2016) Predictive Markers for the Efficacy of Anti-PD-1/PD-L1 Antibodies in Lung Cancer. J Thoracic Oncol 11(7):976–988. https://doi.org/10.1016/j.jtho.2016.02.015
33. Mitra D, Horick NK, Brackett DG, Mouw KW, Hornick JL, Ferrone S, Hong TS, Mamon H, Clark JW, Parikh AR, Allen JN, Ryan DP, Ting DT, Deshpande V, Wo JY (2019) High IDO1 expression is associated with poor outcome in patients with anal cancer treated with definitive chemoradiotherapy. Oncologist 24(6):e275–e283. https://doi.org/10.1634/theoncologist.2018-0794
34. Zhou L, Li Y, Gao W, Huangfu H, Wen S, Zhang C, Zhao Q, Dong Z, Qu C, Li G, Wu L, Wang B (2019) Assessment of tumor-associated immune cells in laryngeal squamous cell carcinoma. J Cancer Res Clin Oncol 145(7):1761–1772. https://doi.org/10.1007/s00432-019-02936-w
35. Herbst RS, Soria JC, Kowanetz M, Fine GD, Hamid O, Gordon MS, Sosman JA, McDermott DF, Powderly JD, Gettinger SN, Kohrt HE, Horn L, Lawrence DP, Rost S, Leabman M, Xiao Y, Mokatrin A, Koeppen H, Hegde PS, Mellman I, Chen DS, Hodi FS (2014) Predictive correlates of response to the anti-PD-L1 antibody MPDL3280A in cancer patients. Nature 515(7528):563–567. https://doi.org/10.1038/nature14011

Affiliations

Junyu Chen[1,3] · Wenlong Zhong[1,3] · Meng Yang[4] · Weibin Hou[1,3] · Xiaofei Wang[1,3] · Kun Xia[1,3] · Hao Yu[1,3] · Meihua Yang[1,3] · Bingkun Zhou[1,3] · Bo Wang[1,3] · Jian Huang[1,3] · Tianxin Lin[1,2,3]

1 Department of Urology, Sun Yat-Sen Memorial Hospital, Sun Yat-Sen (Zhongshan) University, Guangzhou 510120, People's Republic of China

2 Kashgar Prefecture First People's Hospital of Kashi, Xinjiang, People's Republic of China

3 Guangdong Provincial Key Laboratory of Malignant Tumor Epigenetics and Gene Regulation, Sun Yat-Sen Memorial Hospital, Sun Yat-Sen University, Guangzhou, People's Republic of China

4 Department of Urology, Yan' an Hospital of Kunming City, Kunming Medical University, Kunming, People's Republic of China